

# Surface reconstruction from scattered measurements

Ardeshir Goshtasby

Electrical Engineering and Computer Science Department (M/C 154)  
University of Illinois at Chicago  
Chicago, Illinois 60680-4348

## ABSTRACT

Given scattered measurements from a surface, a method for reconstruction of the surface using rational Gaussian surfaces is described. Rational Gaussian surfaces are globally defined parametric surfaces that adapt well to local data. Examples demonstrating reconstruction of 3-D scenes from scattered depth measurements obtained from stereo disparity, reconstruction of 3-D shapes from noisy range data, and segmentation of volumetric images for the extraction of generalized cylinders are described.

## 1. INTRODUCTION

In many computer vision and computer graphics problems, only scattered measurements from a surface are known and there is a need to reconstruct the surface. Surface reconstruction from scattered measurements has been an active area of research for a long time.<sup>1,2</sup> Most methods, however, work on data that are sparsely spaced or are single-valued. Among the methods that can work on dense and multi-valued data, the energy minimizing methods described in references 3-5 may be named. These methods reconstruct surfaces iteratively by minimizing an energy functional. In this paper, surface reconstruction is formulated as a surface fitting problem.

If a single parametric surface can approximate an entire data set, then by changing the parameters of the surface, for example, from 0 to 1, the surface can be reconstructed. A representation should be such that the local shape of a surface is determined from local measurements and the effect of far away measurements on a surface point vanishes rapidly. Such a global representation is introduced in rational form in this paper and called *rational Gaussian (RaG) surfaces*. A RaG surface is defined globally, but is sensitive to local data. The degree of localness of a RaG surface can be controlled by what is known as the *smoothness parameter* of the surface.

A desirable property of RaG surfaces is that the control vertices of a surface do not have to form a regular grid and any arrangement of the control vertices may be used as long as the adjacency relation between them are known. In this paper, RaG surfaces will be used to approximate scattered surface points. The given points will be used as the control vertices of a RaG surface. Since the points may be noisy, approximating rather than interpolating surfaces will be used. In the following, *measurements*, *control vertices*, and *points* will all be used to mean the *given scattered surface points*. In the following, first, the types of data that may be used in the proposed methods are discussed. Then, formulations for open, half-closed, and closed parametric surfaces are given. Next, methods for determination of the knots of a RaG surface from their control vertices are described, and finally, examples of surface reconstruction from scattered measurements are presented.

## 2. THE DATA

Surface measurements that are not given in a regular grid are considered scattered. In many computer vision problem, regularly-spaced image data are not available, and from scattered measurements one must recover the 3-D structure of a scene. Figure 1 shows elevation data obtained by matching high-gradient edges in stereo images of a terrain scene.<sup>6</sup> To reconstruct the terrain in 3-D it is necessary that a surface is fitted to the data.

Figure 2 shows the  $x$ ,  $y$ , and  $z$  coordinates of a panoramic range image of an object obtained by a special range finder (Cyberware 4020 Laser Scanner). The range finder makes a complete revolution about a person's head while

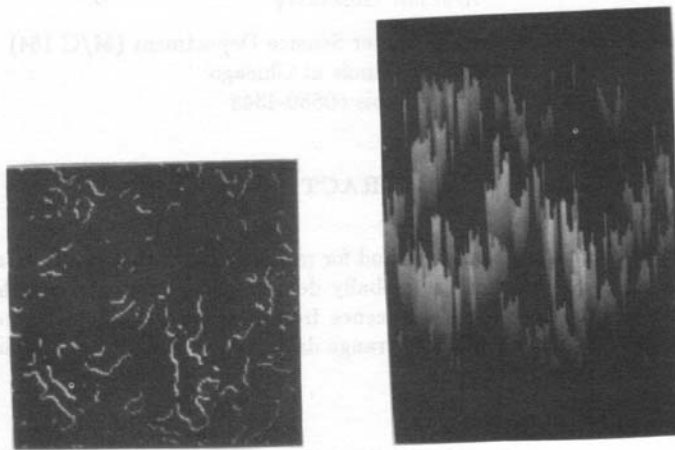


Fig. 1. Elevations of points in a terrain scene obtained by matching stereo images of the scene. (a) Elevation values are represented by intensities with brighter points showing higher elevations. This image is of size  $256 \times 256$ . (b) Same as in (a) except that the heights of the points correspond to their elevations.

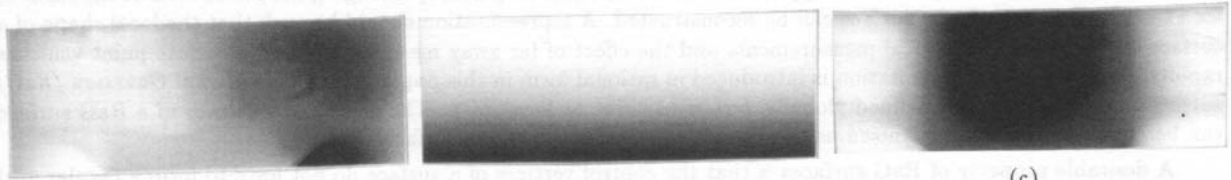


Fig. 2. (a)-(c)  $x$ ,  $y$ , and  $z$  coordinates of points sampled from a person's head by a special range finder (Cyberware 4020 Laser Scanner). These images are of size  $196 \times 512$ .

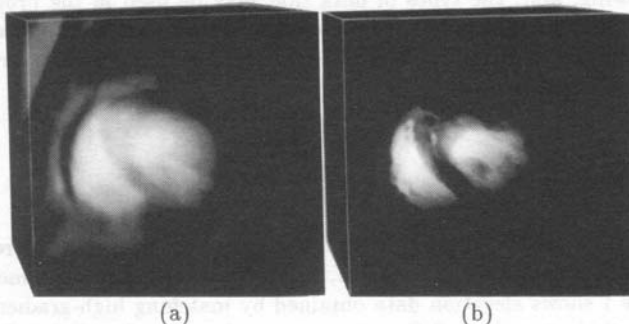


Fig. 3. (a) A volumetric cardiac MR image. (b) Left and right ventricles extracted by segmenting the volumetric image via intensity thresholding. These images are of size  $128 \times 128 \times 50$ .

scanning. Corresponding entries in the three images show the  $x$ ,  $y$ , and  $z$  coordinates of 3-D points on the person's head. From these images, although it appears that uniform measurements are available, but in fact they are not uniform: many points in the images correspond to the same point in 3-D. For instance, many points in the upper rows of the images correspond to the same point on top of the person's head. If repeated points are removed from the images, a set of scattered measurements will be obtained.

Figure 3b shows the left and right ventricles of a human heart obtained by thresholding the intensities in the volumetric cardiac magnetic resonance (MR) image of Fig. 3a. The voxels on the boundary of each of the ventricles represent scattered surface points. These points are used to reconstruct the ventricles.

The given measurements are noisy and a surface representation that fits the measurements should have parameters that can be adjusted to the noise level in the measurements. RaG surfaces can fit to scattered measurements and have smoothness parameters that can be changed to smooth out different levels of noise in an image.

### 3. SURFACE FORMULATIONS

#### 3.1. Open surfaces

An open RaG surface is defined by

$$\mathbf{P}(u, v) = \sum_{i=1}^n \mathbf{V}_i g_i(u, v) \quad u, v \in [0, 1] \quad (1)$$

where

$$g_i(u, v) = \frac{W_i G_i(u, v)}{\sum_{j=1}^n W_j G_j(u, v)} \quad (2)$$

and

$$G_i(u, v) = e^{-[(u-u_i)^2 + (v-v_i)^2]/2\sigma_i^2} \quad (3)$$

In these formulas,  $n$  is the number of control vertices,  $\mathbf{V}_i$  is the  $i$ th control vertex,  $W_i$  is the weight associated with the  $i$ th control vertex,  $(u_i, v_i)$  is the  $i$ th knot, and  $G_i(u, v)$  is a two-dimensional Gaussian centered at  $(u_i, v_i)$  with standard deviation  $\sigma_i$  and height one.  $\sigma_i$  determines the smoothness of the surface in the neighborhood of the  $i$ th knot. If a surface is required to closely follow its control vertices, the standard deviations of the Gaussians (the smoothness parameters) should be given smaller values than when the surface is required to smooth out noisy image data. Since a Gaussian with a larger standard deviation has smaller high-spatial-frequency coefficients, surfaces obtained from Gaussians with larger standard deviations have smaller high-spatial-frequency coefficients. A surface with smaller high-spatial-frequency coefficients is considered *smoother*.

Some of the properties of RaG surfaces are: 1) they are infinitely differentiable everywhere; 2) they fall inside the convex hull of their control vertices; 3) their smoothness parameters may be varied to obtain surfaces that are smooth as well as surfaces that have sharp corners; and 4) the weight associated with a control vertex determines the degree of influence of that control vertex on the surface. A weight could be thought of as the degree of importance of a control vertex. A control vertex with a higher degree of importance should have a greater influence on a surface than a control vertex with a lower degree of importance.

#### 3.2. Half-closed surfaces

Half-closed surfaces are surfaces that are smoothly closed from one side. A generalized cylinder is an example of a half-closed surface. If relation (3) is replaced by

$$G_i(u, v) = \sum_{j=-\infty}^{\infty} e^{-\{[u-(u_i+j)]^2 + (v-v_i)^2\}/2\sigma_i^2} \quad (4)$$

a half-closed surface will be obtained. The infinity in relation (4) comes from the fact that a Gaussian extends from  $-\infty$  to  $\infty$  and when the surface is closed from one side, it makes infinite cycles around the closed side. The effect of

a Gaussian, however, vanishes exponentially, and after a few cycles it may not be measurable by the accuracy of the computer.

Suppose the accuracy of the computer is  $\varepsilon$ ; then in formula (4) when  $e^{-\{[u-(u_i+J)]^2+(v-v_i)^2\}/2\sigma_i^2} < \varepsilon$  the effect of a Gaussian cannot be measured, and that happens when  $J > 1 + \sigma_i\sqrt{-2 \ln \varepsilon}$ . Therefore, only when

$$J \leq \left\lceil 1 + \sigma_i\sqrt{-2 \ln \varepsilon} \right\rceil \quad (5)$$

the effect of a Gaussian on a surface point is measurable. For instance, when  $\varepsilon = 10^{-8}$  and  $\sigma_i = 0.1$ , we find  $J \leq 2$ . With conceivable values of  $\varepsilon$  and  $\sigma_i$ , we find that  $J$  is usually less than 5. Therefore, in practice, the infinity in relation (4) should be replaced by  $J$  determined from (5).

### 3.3 Closed surfaces

A totally closed RaG surface is obtained by replacing relation (3) with

$$G_i(u, v) = \sum_{j=-\infty}^{\infty} \sum_{k=-\infty}^{\infty} e^{-\{[u-(u_i+j)]^2+[v-(v_i+k)]^2\}/2\sigma_i^2}. \quad (6)$$

In practice,  $-J \geq j \leq J$  and  $-K \geq k \leq K$  for some small numbers  $J$  and  $K$  defined by relation (5) and one similar to it for  $K$ .

Note that half-closed and closed RaG surfaces have the same properties as the open RaG surfaces. The existence of the smoothness parameters is especially useful in generating surfaces with different smoothness appearances.

## 4. PARAMETER ESTIMATION

A RaG surface is defined by a set of control vertices  $\{\mathbf{V}_i : i = 1, \dots, n\}$ . Along with each control vertex  $\mathbf{V}_i$ , a weight factor  $W_i$ , a smoothness parameter  $\sigma_i$ , and a knot  $(u_i, v_i)$  should be provided also. To treat all the control vertices equally, one must set all the weights of the surface to the same value. Otherwise, the weights should be taken proportional to the importance of the control vertices. In the next section, examples of both types of weights will be given.

A smoothness parameter determines the smoothness of a generated surface in the neighborhood of the corresponding knot. If measurements in a neighborhood are known to be noisy, the smoothness parameters in that neighborhood should be increased to smooth out the noise. If measurements are not noisy, smaller smoothness values should be used to allow the surface to follow the measurements closely. If it is desired to treat all areas in a surface similarly, all smoothness parameters should be given the same value so that the smoothness of the entire surface could be changed with a single parameter. If an application allows user interaction, then this parameter may be interactively varied until a desired smoothness is obtained in a reconstructed surface.

Given scattered points from a surface, a process is required that can determine the adjacency relation between the points. By connecting adjacent points on a surface, a polyhedral approximation to the surface can be obtained. In parametric surfaces, this adjacency information is embedded in the knots of the surface. For some data sets, the adjacency relation between points can be determined from the given data. For others, determination of the adjacent relation from the data is a complex task. This problem has been studied by Hoppe *et al.*<sup>7</sup>

Image of Fig. 1 shows single-valued data whose knots can be estimated from the  $x$  and  $y$  coordinates of the data points. Assuming the image is of size  $m \times n$  with rows numbered from 0 to  $(m - 1)$  and columns numbered from 0 to  $(n - 1)$ , the knot to be associated with the  $i$ th data point is computed from

$$u_i = \frac{x_i}{m - 1}, \quad v_i = \frac{y_i}{n - 1}, \quad (7)$$

where  $x_i$  and  $y_i$  are the row and column numbers of the  $i$ th data point in the image.

Figure 2 shows three images representing the  $x$ ,  $y$ , and  $z$  coordinates of points in 3-D. The scanner that obtains this kind of data makes a complete revolution about an object while scanning. The row numbers in these images correspond to the height, and the column numbers in a given row show the angle of rotation of the scanner. Assuming  $j$  denotes the rows, varying from 0 to  $(m - 1)$ ;  $k$  denotes unique points in row  $j$ , varying from 0 to  $(n_j - 1)$ ; and the  $k$ th point in the  $j$ th row represents the  $i$ th measurement; then  $(u_i, v_i)$  is computed from

$$u_i = \frac{k}{n_j}, \quad v_i = \frac{j}{(m - 1)}. \quad (8)$$

Note that the number of unique points in row  $j$  depends on the index of the row. For example, in Fig. 2 there are fewer unique points in the top rows than around the center of the image. In relation (8) since the surface closes,  $u_i$  is formulated such that when  $u_i$  is equal to 0 or 1 the same surface point is obtained.

If only a window from images in Fig. 2 is used, the obtained surface will not be closed. In that case, the knots of the surface should be computed from

$$u_i = \frac{k}{(n_j - 1)}, \quad v_i = \frac{j}{(m - 1)}, \quad (9)$$

where  $m$  is the number of rows in the window and  $n_j$  is the number of unique points in the  $j$ th row.

The image of Fig. 3a shows transformation of a sequence of cardiac MR slices into the volumetric representation,<sup>8</sup> and Fig. 3b shows segmentation of the image by intensity thresholding. Image slices parallel to the  $xy$ -plane correspond to image slices that are either scanned by the MR scanner or generated by an interpolation process to obtain an isotropic volume data.<sup>8</sup> Traveling through this volume data along the  $z$ -axis we will go through different image slices. In each slice, two closed contours are obtained that correspond to the left and right ventricular boundaries. The number of boundary points on each ventricle changes from one slice to another. Assuming  $j$  denotes the slice numbers varying from 0 to  $(m - 1)$ , and  $k$  denotes the pixel numbers on a boundary contour in slice  $j$ , varying from 0 to  $(n_j - 1)$ , the knot to be associated with the  $k$ th boundary point in the  $j$ th slice is determined by formula (8). Since data of Fig. 3 represent two separate objects, each object is represented by a half-closed RaG surface with the parametrization of (8).

Data of Figs 2 and 3 show generalized cylinders. In Fig. 2, the axis of the cylinder is a straight line normal to the  $xz$  plane, while in Fig. 3 the axes of the cylinders bend with the data. Any elongated object from which scattered measurements are available at scans along the axis of the object can be reconstructed with a half-closed RaG surface and parametrization of (8). Note that if the first scan follows the last in a generalized cylinder, a totally closed surface will be obtained. Assuming the  $k$ th sample point in the  $j$ th scan represents the  $i$ th measurement, the  $i$ th knot of a generalized cylinder that closes smoothly, like a torus, can be determined from

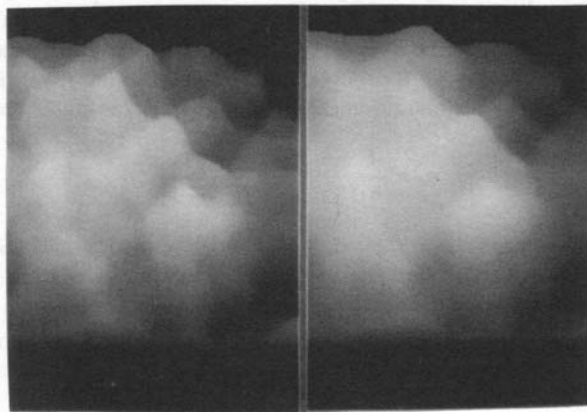
$$u_i = \frac{k}{n_j}, \quad v_i = \frac{j}{m}. \quad (10)$$

In the following, RaG surfaces with parameters as determined above will be used to reconstruct surfaces from scattered measurements.

## 5. RESULTS

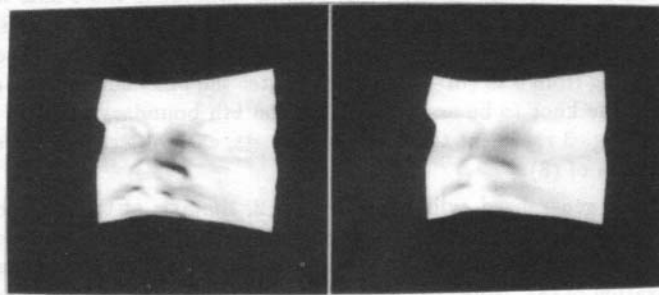
In the first experiment, non-zero points in Fig. 1 were used as the control vertices of an open RaG surface. In equation (3), the standard deviations of all Gaussians were set to  $\sigma$  so that the smoothness appearance of the entire surface could be controlled by a single parameter. Using equal weights, and knots as defined by (7), the surfaces of Figs 4a and 4b were obtained with  $\sigma$  equal to 0.04 and 0.06, respectively.

Next, another open surface was generated by taking a small window off the images of Fig. 2. The upper-left-hand corner of the window was at (50, 150) in the images and the window size was  $72 \times 128$ . Using formula (1) with equal weights, equal standard deviations of Gaussians, and knots as computed by (9), the surfaces of Fig. 5 were obtained. Figures 5a and 5b are surfaces obtained by setting standard deviations of all Gaussians equal to 0.15 and



(a) (b)

Fig. 4. (a)-(b) Reconstruction of the terrain scene by fitting an open RaG surface to the data of Fig. 1b with standard deviations of all Gaussians equal to 0.04 and 0.06, respectively. All weights were taken to be the same and the knots of the surface were computed from (7).



(a) (b)

Fig. 5. Reconstruction of the face from the data of Fig. 2. A  $72 \times 128$  window was extracted from the images and used as the  $x$ ,  $y$ , and  $z$  coordinates of scattered points from the face. Repeated points were removed and only unique points were used in the approximation. The standard deviations of all Gaussians were set to (a) 0.15 and (b) 0.3.

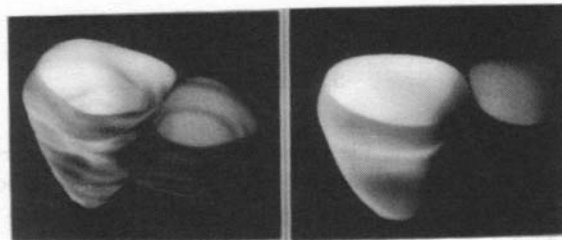


Fig. 7.

Fig. 6. Reconstruction of the head by fitting a half-closed RaG surface to the data of Fig. 2 with equal weights and knots as obtained by (8). The standard deviations of all Gaussians used in this experiment were 0.3.

0.3, respectively. When the standard deviations of Gaussians are small, noise in the measurements appear in the reconstructed surface. By increasing the standard deviations, noise in the measurements smooth out and a pleasing surface is obtained as shown in Fig. 5b. Further increase in the standard deviations of Gaussians smoothes the face features and would not be appropriate.

Using the entire data of Fig. 2 with formulation of the half-closed surface, and using equal weights, standard deviations of all Gaussians equal to 0.3, and knots as defined by (8), the surface of Fig. 6 was obtained.

The voxels on the boundaries of the ventricles shown in Fig. 3b were approximated by two half-closed surfaces. The weight at a voxel was taken to be equal to the 3-D gradient magnitude<sup>9</sup> at the voxel. Weights were selected in this manner because a point corresponding to a higher gradient magnitude shows a boundary point with a higher level of confidence than a point with a lower gradient magnitude. Computing the knots of the surface from (8) and setting the standard deviations of all Gaussians equal to 0.02, the surfaces shown in the left side of Fig. 7 were obtained. Increasing the standard deviations of the Gaussians to 0.05, the surfaces in the right side of Fig. 7 were obtained.

We did not have real data from a totally closed surface; therefore, 100 random points were sampled from a torus. The knots at the points were taken proportional to the angles of the points along and around the major axis of the torus. Using a closed RaG surface with equal weights and standard deviations of all Gaussians equal to 0.1, the surface of Fig. 8 was obtained as an approximation to the torus.

## 6. CONCLUDING REMARKS

The shape of a RaG surface depends not only on the provided control vertices but also on the provided knots, weights, and standard deviations of Gaussians. Increasing the weight at a control vertex will pull the surface towards that control vertex. Since RaG surfaces are in rational form, multiplying all the weights by the same amount will have no effect on the surface. The weights in a RaG surface should be taken proportional to the relative importance of the measurements from which a surface should be constructed. The shape of a parametric surface changes with its knots. In this paper, methods for estimation of knots for three types of data were described. These knots may further be optimized by an iterative process described by Sarkar and Menq.<sup>10</sup>

The standard deviations of Gaussians also change the shape of a generated surface. By increasing the standard deviations of Gaussians a smoother surface is obtained. Larger standard deviations should be used when noise in the measurements are significant. If data are not noisy and the surface to be generated has to follow the data closely, smaller standard deviations should be used. Standard deviations in a surface may be set to a common parameter so that the shape of an entire surface could be controlled with a single parameter. The proper value of the common standard deviation may be determined either interactively by changing its value and observing the shape of the obtained surface, or automatically by iteratively varying its value until a minimum is reached in an error criterion.

A remarkable property of RaG surfaces is that they can be smooth in one area while having sharp corners in another. This property is realized when large standard deviations are assigned to control vertices where a smooth area is required while assigning small standard deviations to control vertices where sharp corners are required.

In the preceding sections, methods for reconstruction of surfaces from scattered measurements were described. The methods were tested on different types of data and the results were presented. For other types of data, the major challenge would be to estimate the knots or determine the adjacency relation between the data points.

In the examples described above, a single surface was used to represent each data set. Therefore, by changing parameters  $u$  and  $v$  of a surface from 0 to 1 the entire surface could be drawn. Implementation of RaG surfaces ~~is~~<sup>is</sup> very easy. The entire program generating open, half-closed, and closed surfaces from scattered measurements is listed in one page in the Appendix.

## ACKNOWLEDGEMENTS

The author would like to thank Dr. David A. Turner of MRI at Presbyterian-St. Luke's Hospital for providing the MR image of Fig. 3a and Mr. Paul Neumann of Biomedical Visualization Laboratory at University of Illinois at

Chicago for providing the range image of Fig. 2 for this study. The help of Bavani Ramanan in generation of images of Figs 5-8 is also greatly appreciated.

Fig. 6.

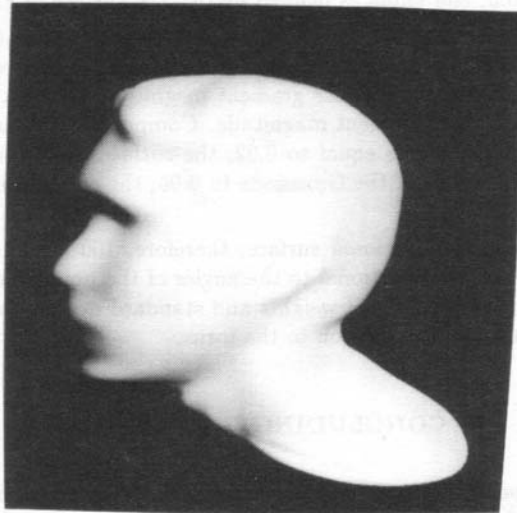


Fig. 7. Two half-closed RaG surfaces fitting points on the ventricular boundaries of Fig. 3b. The weights associated with the points were taken to be equal to the 3-D gradient magnitudes of the points, and the knots of the surfaces were computed from (8). The surfaces are obtained by setting the standard deviations of all Gaussians to 0.02 (in the left image) and 0.05 (in the right image).

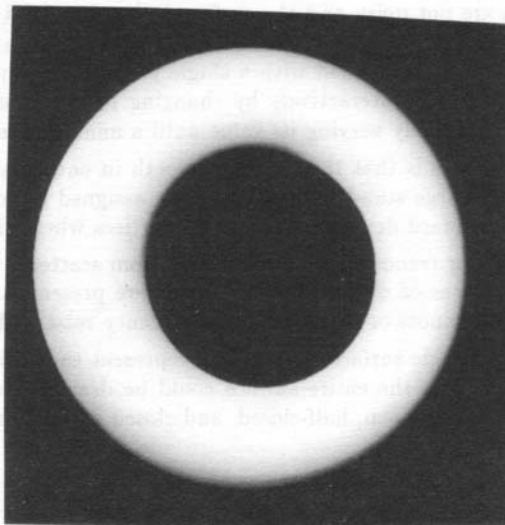


Fig. 8. A torus reconstructed from 100 scattered points. Weights at all the points were set to the same value, and  $u_i$  and  $v_i$  were taken proportional to the angular bends of the  $i$ th point along and around the major axis of the torus. Standard deviations of all Gaussians were 0.1.

## REFERENCES

1. R. Franke and L. L. Schumaker, "A bibliography of multivariate approximation," in *Topics in Multivariate Approximation*, C. K. Chui, L. L. Schumaker, and F. I. Utceras (eds.), Academic Press, pp. 275-335, 1987.
2. E. Grosse, "A catalogue of algorithms for approximation," in *Algorithms for Approximation II*, J. C. Mason and M. G. Cox (Eds.) Chapman and Hall, New York, pp. 479-514, 1990.
3. D. Terzopoulos, A. Witkin, and M. Kass, "Energy constraints on deformable models: recovering shape and non-rigid motion," *Proc. 6th Nat. Conf. Artificial Intelligence, AAAI-87*, Seattle, WA, pp. 755-760, July 1987.
4. R. Szeliski and D. Terzopoulos, "From splines to fractals," *Computer Graphics*, vol. 23, no. 3, pp. 51-60, 1989.
5. L. D. Cohen, "On active contour models and balloons," *Image Understanding*, vol. 53, no. 2, pp. 211-218, 1991.
6. A. Goshtasby, "Stereo correspondence by selective search," *Proc. Japan Computer Vision Conference*, Tsukuba, Japan, pp. 1-10, July 1989.
7. H. Hoppe, T. DeRose, T. Duchamp, J. McDonald, and W. Stuetzle, *Surface reconstruction from unorganized points*, TR# 91-12-03, Department of Computer Science and Engineering, University of Washington, 1991.
8. A. Goshtasby, D. A. Turner, and L. V. Ackerman, "Matching of tomographic image slices for interpolation," to appear in *IEEE Trans. Medical Imaging*.
9. S. W. Zucker and R. A. Hummel, "A three-dimensional edge operator," *IEEE Trans. Pattern Analysis and Machine Intelligence*, vol. 3, no. 3, pp. 324-331, 1981.
10. B. Sarkar and C-H Menq, "Parameter optimization in approximating curves and surfaces to measurement data," *Computer Aided Geometric Design*, vol. 8, pp. 267-290, 1991.

## APPENDIX

```

/* The following code implements relations (1)-(4) and (6) */
/* in the paper. */

double *x, *y, *z, *t1, *t2, *w, *sigma;

/* Global parameters:
/* x[], y[], z[] are one-dimensional arrays dynamically allocated */
/* to hold the x, y, and z coordinates of the measurements, */
/* (t1[], t2[]) show the knots, w[] show weights at the */
/* measurements, and sigma[] show the stiffness parameters. */

double esup(u,v,i,j,k)
double u,v; /* This procedure computes the */
int i,j,k; /* value of one term in (6). */
{ double t3,t4,r1,r2,r; /* When k=0, it evaluates a term */
  t3=j; t4=k; /* in (4), and when j=0 and k=0 */
  r1=u-(t1[i]+t3); /* it evaluates (3). */
  r2=v-(t2[i]+t4);
  r=(r1*r1+r2*r2)/(2.0*sigma[i]*sigma[i]);
  if(r<40.0) r=exp(-r); else r=0.0;
  return(r);
}

double sumesup(u,v,i,jj,kk)
double u,v; /* This procedure evaluates relation */
int i,jj,kk; /* (6), when kk=0; it evaluates */
{ double sum; /* relation (4), and when jj=0. it */
  int i1,i2,j,k; /* evaluates relation (3). */
  sum=esup(u,v,i,0,0);
  for(j=1; j<jj; j++)for(k=1; k<kk; k++)
  sum=sum+esup(u,v,i,j,k)+esup(u,v,i,-j,k)
  +esup(u,v,i,j,-k)+esup(u,v,i,-j,-k);
  return(sum);
}

double denum(u,v,jj,kk)
double u,v; /* This procedure determines the */
int jj,kk; /* denominator of relation (2). */
{ int i;
  double sum;
  sum=0.0;
  for(i=0; i<n; i++) sum=sum+w[i]*sumesup(u,v,i,jj,kk);
  return(sum);
}

double findg(u,v,i,jj,kk)
double u,v; /* This procedure evaluates */
int i,jj,kk; /* relation (2). */
{ double d;
  d=w[i]*sumesup(u,v,i,jj,kk)/denum(u,v,jj,kk);
  return(d);
}

void findp(u,v,jj,kk,px,py,pz)
double u,v; /* This procedure evaluates */
int jj,kk; /* relation (1). */
double *px,*py,*pz; /* px, py, and pz are the */
{ double s,sumx,sumy,sumz,d; /* x, y, and z coordinates */
  int i; /* of a point on an open */
  d=denum(u,v,jj,kk); /* (when jj=0 and kk=0), */
  sumx=0.0; sumy=0.0; sumz=0.0; /* half-open (when kk=0), */
  for(i=0; i<n; i++) /* and closed surface. */
  { s=w[i]*sumesup(u,v,i,jj,kk); /* jj (J) can be computed */
    sumx=sumx+x[i]*s; /* from relation (5), and */
    sumy=sumy+y[i]*s; /* kk may be computed from */
    sumz=sumz+z[i]*s; /* a similar relation. */
  }
  sumx=sumx/d; sumy=sumy/d; sumz=sumz/d;
  (*px)=sumx; (*py)=sumy; (*pz)=sumz;
}

```